JOURNAL OF VIROLOGY, Nov. 2011, p. 11655–11663 Vol. 85, No. 22
0022-538X/11/$12.00 doi:10.1128/JVI.05644-11

Evidence for an Increased Risk of Transmission of Simian Immunodeficiency Virus and Malaria in a Rhesus Macaque Coinfection Model▽†

Kristin A. Trott,[1] Jennifer Y. Chau,[2] Michael G. Hudgens,[3,4] Jason Fine,[4] Chelu K. Mfalila,[3] Ross P. Tarara,[1] William E. Collins,[5] JoAnn Sullivan,[5] Shirley Luckhart,[2] and Kristina Abel[6]*

California National Primate Research Center, University of California at Davis, County Road 98/Hutchison Drive, Davis, California 95616[1]; Department of Medical Microbiology and Immunology, University of California at Davis, One Shields Avenue, Davis, California 95616[2]; Center for AIDS Research, Lineberger Comprehensive Cancer Center, CB 7295, University of North Carolina at Chapel Hill, Chapel Hill, North Carolina 27599-7295[3]; Department of Biostatistics, McGavran-Greenberg Hall, CB 7420, University of North Carolina at Chapel Hill, Chapel Hill, North Carolina 27599-7420[4]; Centers for Disease Control and Prevention, Center for Global Health, Division of Parasitic Diseases and Malaria, 1600 Clifton Road, Atlanta, Georgia 30333[5]; and Department of Microbiology and Immunology, School of Medicine, University of North Carolina at Chapel Hill, 120 Mason Farm Rd., CB 7042, Chapel Hill, North Carolina 27599-7042[6]

Received 10 July 2011/Accepted 31 August 2011

In sub-Saharan Africa, HIV-1 infection frequently occurs in the context of other coinfecting pathogens, most importantly, *Mycobacterium tuberculosis* and malaria parasites. The consequences are often devastating, resulting in enhanced morbidity and mortality. Due to the large number of confounding factors influencing pathogenesis in coinfected people, we sought to develop a nonhuman primate model of simian immunodeficiency virus (SIV)-malaria coinfection. In sub-Saharan Africa, *Plasmodium falciparum* is the most common malaria parasite and is responsible for most malaria-induced deaths. The simian malaria parasite *Plasmodium fragile* can induce clinical symptoms, including cerebral malaria in rhesus macaques, that resemble those of *P. falciparum* infection in humans. Thus, based on the well-characterized rhesus macaque model of SIV infection, this study reports the development of a novel rhesus macaque SIV-*P. fragile* coinfection model to study human HIV-*P. falciparum* coinfection. Using this model, we show that coinfection is associated with an increased, although transient, risk of both HIV and malaria transmission. Specifically, SIV-*P. fragile* coinfected macaques experienced an increase in SIV viremia that was temporarily associated with an increase in potential SIV target cells and systemic immune activation during acute parasitemia. Conversely, primary parasitemia in SIV-*P. fragile* coinfected animals resulted in higher gametocytemia that subsequently translated into higher oocyst development in mosquitoes. To our knowledge, this is the first animal model able to recapitulate the increased transmission risk of both HIV and malaria in coinfected humans. Therefore, this model could serve as an essential tool to elucidate distinct immunological, virological, and/or parasitological parameters underlying disease exacerbation in HIV-malaria coinfected people.

HIV and malaria represent two of the most serious health problems. Worldwide, *Plasmodium* species are responsible for 300 to 600 million clinical malaria episodes and 1.2 million deaths annually (23). Most of the malaria-associated deaths can be attributed to infection with *Plasmodium falciparum*, the parasite most common in sub-Saharan Africa. Sub-Saharan Africa is also the epicenter of the HIV pandemic, with more than 20 million HIV-1-infected people (44). The geographical overlap urges a combined effort in combating both diseases. Importantly, there is a need to understand how both pathogens interact with each other and alter host immune responses in coinfected individuals.

The clinical and epidemiological importance of coinfection with HIV and *P. falciparum* has been disputed. Initial studies did not find increases in morbidity and HIV transmission due to coinfection and concluded that coinfection was only a geographical coincidence (8). More recent data, however, suggest that HIV-1-infected people are at greater risk for severe malaria and, conversely, that malaria episodes in HIV-1-infected people result in increased viremia and morbidity (5, 12, 20, 22, 24, 27, 28, 47, 50). Mathematical models estimate that enhanced malaria incidence due to HIV-1 infection translates into an additional 3 million malaria cases and 65,000 deaths

* Corresponding author. Mailing address: Department of Microbiology and Immunology and Center for AIDS Research, School of Medicine, University of North Carolina at Chapel Hill, Genetic Medicine Bldg., Rm. 2047, 120 Mason Farm Rd., CB 7042, Chapel Hill, NC 27599-7042. Phone: (919) 843-9560. Fax: (919) 966-6870. E-mail: abelk@med.unc.edu.

† Supplemental material for this article may be found at http://jvi.asm.org/.

▽ Published ahead of print on 14 September 2011.

due to HIV-1 annually (27). A similar modeling approach predicted that coinfection in Kenya had resulted in an excess of 8,500 HIV-1 infections and 980,000 malaria infections since 1980 (3).

Multiple confounding factors will influence the outcome of coinfection: age, time of coinfection (acute or chronic phase of HIV infection), preexisting immunity to malaria (areas of stable versus unstable transmission), degree of HIV-1-induced immunosuppression, and dysfunction of immune cells due to malaria infection. A relevant animal model would facilitate better definition of pathogen interactions and identification of immune mechanisms leading to disease exacerbation in coinfected animals under controlled conditions. Recently, Koehler et al. showed in a nonhuman primate model of simian immunodeficiency virus (SIV) and *Plasmodium cynomolgi* infection that coinfected animals experienced acceleration to simian AIDS and impaired antimalarial immune responses (26). Clinically, infection with *P. cynomolgi* closely reflects symptoms of human *Plasmodium vivax* infection. Considering that the majority of HIV-1 and malaria infections occur in sub-Saharan Africa, we sought to develop a rhesus macaque SIV-malaria coinfection model that would more closely mimic human HIV-1–*P. falciparum* coinfection. Among the primate malarias, four species are recognized as "falciparum-like": the type species *P. falciparum*, *Plasmodium coatneyi*, *Plasmodium fragile*, and *Plasmodium reichenowi* (11). While a gametocyte-producing strain of *P. falciparum* was developed and was shown to be infective for *Aotus* spp. (14, 37, 52), New World monkeys, which include *Aotus*, are in general less susceptible than are Old World species to SIV infection (25, 34). Similarly, *P. reichenowi* infects only anthropoid apes (e.g., chimpanzees, gorillas). Among the falciparum-like species, only *P. coatneyi* and *P. fragile* can infect *Macaca mulatta.* Blood-induced infections with *P. coatneyi* in *M. mulatta*, however, can result in rapid death in a large proportion of infected animals (11). In contrast, *P. fragile* infection is more readily controlled (11). Further, *P. fragile* can be continuously cultured *in vitro* (9) and, therefore, has been more frequently used for drug and vaccine studies than has *P. coatneyi* (4, 15, 21, 43). Lastly, *P. fragile* is not infectious to humans (49), which is an important consideration for biosafety management. Although *P. fragile* and *P. falciparum* are only distantly related and the course of *P. fragile* infection in its natural simian host has not been extensively studied, we chose the simian parasite *P. fragile*, because *P. fragile* can, similar to *P. falciparum* in humans, induce a nonrelapsing disease and cerebral malaria in rhesus macaques (21).

In the current study, we present a novel rhesus macaque SIV-*P. fragile* coinfection model. Our data demonstrate a transient increase in SIV viremia during acute malaria infection and increased gametocytemia in the blood of SIV-*P. fragile*-coinfected animals that results in enhanced oocyst frequencies in mosquitoes. These results support epidemiological data that HIV-malaria coinfection in humans can result in an increased, although transient, risk of transmission of both HIV-1 and malaria (5, 24, 28, 46). Furthermore, we show that increased viremia is associated with malaria-induced immune activation. Thus, the rhesus macaque model of SIV-*P. fragile* coinfection could serve as an important tool to better understand comorbidity and thereby lead the way to novel therapeutic interventions.

MATERIALS AND METHODS

Animals and infections. Adult male rhesus macaques were obtained from and housed in accordance with the regulations of the American Association for Assessment and Accreditation of Laboratory Animal Care (AAALAC) at the California National Primate Research Center (CNPRC). Three groups of animals were included in the study. SIV infections ($n = 2$) were established via intravenous (i.v.) inoculation with 10^3 50% tissue culture infective doses ($TCID_{50}$s) of SIVmac239. Malaria infections ($n = 3$) were performed via i.v. inoculation with 1×10^6 to 2×10^6 *P. fragile*-infected rhesus macaque erythrocytes prepared according to *Methods in Malaria Research* (29). In order to establish chronic malaria, animals were treated with 150 mg quinine sulfate (Qualaquin; URL Pharma, Inc., Philadelphia, PA) via orogastric intubation for 2 consecutive days when parasitemia rose above 0.5%. SIV-*P. fragile* coinfected animals ($n = 6$) were inoculated with SIV 28 days prior to inoculation with *P. fragile* and treated with 150 mg quinine sulfate for 2 or 4 consecutive days (see Results). For clarity and comparative analysis, all time points are reported based on the time of SIV infection. Thus, day 0 corresponds to the time of SIV infection in SIV-only and SIV-*P. fragile*-coinfected animals. Day 28 corresponds to the time of *P. fragile* infection in SIV-*P. fragile*-coinfected animals and to the time of *P. fragile* infection in *P. fragile*-only infected animals. For clarity, days postinoculations with *P. fragile* are also listed.

During the acute stage of malaria infection, blood was collected every other day to monitor hematocrit, parasitemia, and infectivity to mosquitoes. Thereafter, blood samples were collected weekly for parasitologic, virologic, immunologic, and infectivity analyses. At necropsy, lymphoid tissues, liver, and brain were collected for histological analysis of parasite presence.

DNA and RNA isolation. DNA or RNA was extracted from 250 μl whole EDTA blood collected in 1:3 in TRIzol LS (Invitrogen, Carlsbad, CA) according to the manufacturer's protocol. DNA and RNA samples were stored at −20°C and −80°C, respectively.

Viral load measurement. Plasma RNA samples were analyzed for viral RNA by a quantitative reverse transcrition-PCR (qRT-PCR) assay as described elsewhere (10). Results are reported as viral RNA copies per ml of plasma.

Parasitemia measurement. Parasitemia and gametocytemia were assessed by thin smears of peripheral blood stained with Giemsa stain in a total of approximately 200 fields. Parasitemia is reported as a percentage of infected erythrocytes (infected red blood cells [iRBC]), asexual plus sexual stages, compared to the total erythrocyte number, while gametocytemia is the percentage of sexual stage-infected erythrocytes compared to the total infected erythrocyte number.

Considering that *P. falciparum* can be sequestered and that low *P. fragile* parasitemia might be difficult to detect in thin blood smears, a quantitative PCR assay based on the sequence of the 18S ribosomal subunit (GenBank M61722) of *P. fragile* was developed for parasite detection in tissues and to test blood samples that were negative by microscopic blood smear analysis. The sequences of forward and reverse primers and TaqMan probe were as follows: forward, 5′-CAGCTTTTGATGTTACGGGTATTG-3′; reverse, 5′-CCTCTCCGGAATCGAACTCTAA-3′; probe, 5′-CCTAACATGGCTATGACGGGTAACGGG-3′. PCR was performed using 100 ng DNA, 300 nM primers, and 200 nM probe in a total volume of 25 μl with the 7900 ABI default PCR amplification program. A plasmid clone of *P. fragile* 18S DNA was used as a positive control, and no-template negative controls were included in each reaction set. In addition, template DNA quality was confirmed by amplification of rhesus macaque CCR5 for each sample. Data were quantified via comparison to a plasmid standard curve and are reported as copies/μg total DNA. The assay sensitivity limit was 10 copies/μg DNA. Based on the original blood volume used for DNA isolation and the number of erythrocytes per microliter of blood available through a differential blood count, parasitemia could then be reported as percent *P. fragile*-infected erythrocytes.

PCR was also developed for the detection of the sexual stage of *P. fragile*. To quantify gametocytes in the peripheral blood, we developed a qRT-PCR assay based on the gametocyte-specific gene 230. Because the sequence of *P. fragile* 230 was unknown, we aligned the known sequences from *P. vivax*, *P. falciparum*, *Plasmodium knowlesi*, *Plasmodium chabaudi*, and *Plasmodium yoelii* (PF-230_XM_001349564, PV-230_XM_001612970, PB-230_XM_672775, PC-230_XM_739974, and PY-230_XM_002257909) and developed primers in conserved regions based on the *P. vivax* sequence (AGAAATTCCGAGTGTGGTGAGC, nucleotides 3579 to 3591, and CTTTGTTGTAGCCCTCCCCTTT, nucleotides 3703 to 3724). PCR was performed using 1× AmpliTaq mastermix (Applied Biosystems), 1.25 U AmpliTaq polymerase, 0.5 μM primers, 200 μM deoxynucleoside triphosphates, and 300 ng DNA in a total reaction volume of 50 μl. We amplified DNA from *P. fragile*-infected rhesus macaque blood samples on a Veriti thermal cycler (Applied Biosystems, CA) under the following conditions:

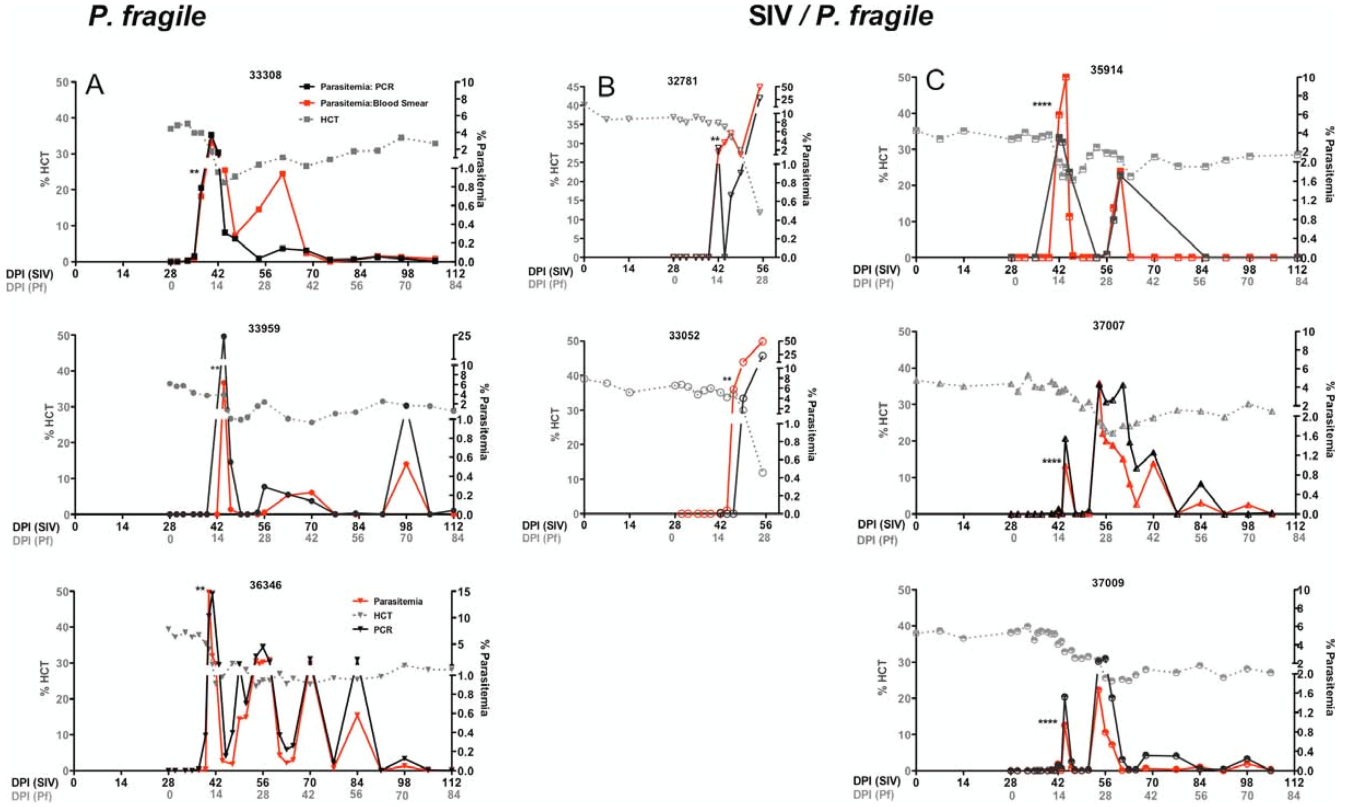

FIG. 1. *P. fragile* and SIV-*P. fragile* animal models. The data show the correlation between hematocrit (dotted line) and parasitemia, measured as the percentage of infected RBC per total RBC by blood smear (solid red line) or as total copies of *P. fragile* DNA per total RBC by PCR analysis (solid black line) in *P. fragile*-infected (A) and SIV-*P. fragile*-coinfected (B and C) animals. Asterisks indicate the time of quinine sulfate treatment. A 2-day treatment effectively induced chronic parasitemia in *P. fragile*-only-infected (A), but not in SIV-*P. fragile*-coinfected (B) animals. (C) Chronic parasitemia in SIV-*P. fragile*-coinfected animals was induced by a 4-day quinine sulfate treatment.

denaturation at 94°C for 3 min, 40 cycles of amplification (94°C for 30 s, 56°C for 30 s, and 70°C for 30 s) and a terminal extension at 70°C for 10 min. Subsequently, we isolated the gene product by using the QIAquick gel extraction kit (Qiagen, CA), cloned the fragment into a plasmid (TOPA TA cloning kit; Invitrogen, CA), and sequenced the plasmid (Davis Sequencing, Davis, CA). *P. fragile*-specific primers (forward, 39, CATAAATGGTATCCAATAGCTTT GCA; reverse, 136, AGCAAAGATCTGTCGTTCAAATGT) and probe (86, CGTCAACGTGTACTCCTTCTTCAAAAGTACACACA) were then developed.

RNA isolated from whole blood was reverse transcribed into cDNA as described previously (1, 2), and real-time PCR was performed with 100 ng of cDNA using the ABI default program. The plasmid clone of *P. fragile* 230 was used as a positive control, and no-template negative controls were included in each reaction. Data were quantified via comparison to a plasmid standard curve and reported as copies/μl blood. Note that samples that tested negative for gametocytemia by blood smear analysis also did not result in detection by gametocyte-specific genes by PCR, confirming the specificity of the observed sequences.

Mosquito husbandry and feeding. Laboratory-reared adult female *Anopheles freeborni* were used for transmission studies as described previously (16). For each assay, a carton of 100 female mosquitoes was provided access to 1 ml of heparinized, freshly drawn, warm peripheral blood from a *P. fragile*-infected or SIV-*P. fragile*-coinfected animal via an artificial feeding apparatus. Following blood feeding, mosquitoes were provided with 10% sucrose-soaked cotton pads. Non-blood-fed mosquitoes were removed from the cartons, and the remaining mosquitoes were maintained at 28°C with 80% humidity for 10 to 12 days. After this time, midguts were dissected from mosquitoes with mature eggs (indicative of complete engorgement) and stained with 1% mercurochrome to count *P. fragile* oocysts (19). Mosquito infectivity is reported as the percentage of mosquitoes with at least 1 oocyst relative to the total number of blood-fed mosquitoes.

Tissue H&E staining. For light microscopy, tissues were fixed in 10% buffered neutral formalin for 24 h and then stored in 70% ethanol until paraffin embedding. Tissues were sectioned at 4 μm and stained with hematoxylin and eosin (H&E).

Phenotypic characterization of lymphocyte populations. Multiparameter flow cytometric analyses were performed to characterize lymphocyte populations in whole peripheral blood. All antibodies were from BD Biosciences (San Jose, CA). T cell activation and proliferation of CD4-positive T cells (CD3 clone SP34-2 and CD4 clone L200) were defined by using antibodies to CCR5 (clone 3A9) and to Ki67 (clone B56), respectively. Samples were acquired on a FACS ARIA apparatus (Beckton-Dickinson), and data were analyzed using FlowJo software (TreeStar; Ashland, OR) as described previously (30, 48). Data are reported as the frequency of $CD3^+$ $CD4^+$ lymphocytes that stained positive for an individual marker.

Measurement of plasma NO and cytokine levels. Plasma nitric oxide (NO) levels were measured using the QuantiChrom nitric oxide assay by BioAssay Systems (Hayward, CA) according to the manufacturer's protocol. Undiluted plasma samples were assayed in duplicate, and average data are reported as μM NO in plasma. Levels of gamma interferon (IFN-γ) and interleukin-6 (IL-6) in plasma were determined using the Th1/Th2 nonhuman primate bead array (Beckton-Dickinson).

Statistical analysis. To assess differences in virologic outcomes between SIV-only ($n = 7$) and SIV-*P. fragile*-coinfected animals ($n = 5$), we compared levels of SIV replication from 4 weeks post-SIV infection (p.i.), the time of *P. fragile* infection, until after resolution of primary parasitemia. Specifically, as primary parasitemia generally became detectable between days 10 and 14 p.i. with *P. fragile*, the slope of viral RNA between days 42 and 56 p.i. with SIV-SIV was compared with the exact Wilcoxon rank-sum test. Estimates of slopes were obtained from a linear model using all available plasma RNA values from days 42 to 56. Day 28 plasma RNA values were imputed for day 42 for 2 animals in

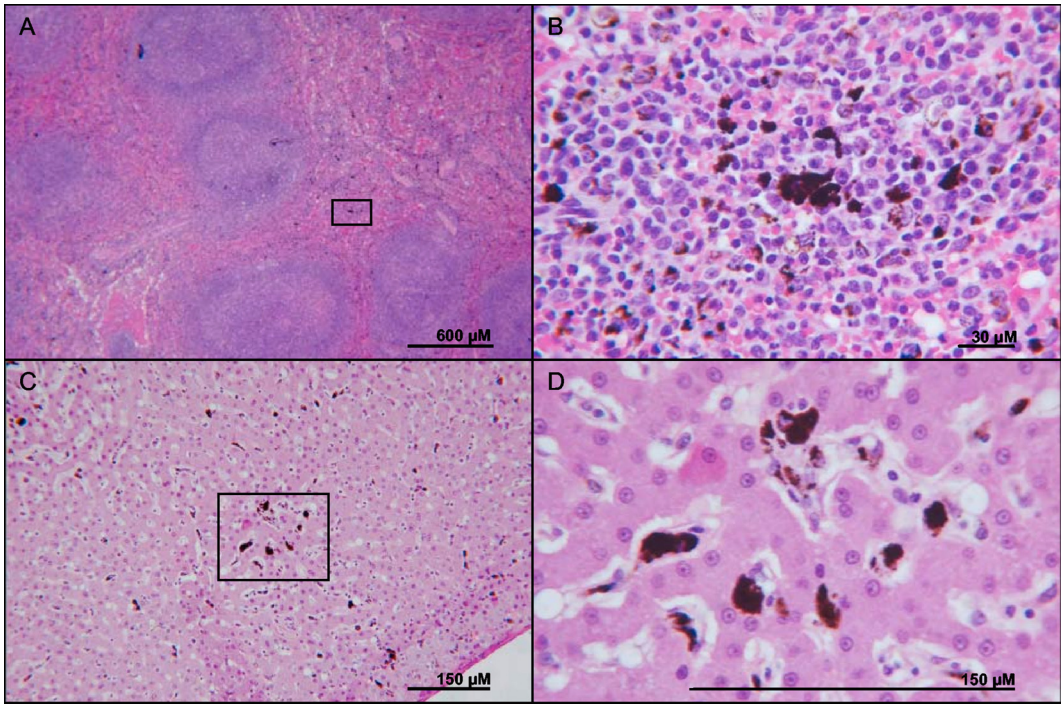

FIG. 2. Pathological changes associated with coinfection. Shown are the spleen (A and B) and liver (C and D) from a representative SIV-*P. fragile*-coinfected animal. (A) Several large closely apposed secondary lymphoid follicles with pale germinal centers were present in the red white pulp of the spleen, while dark brown to black hemozoin was disseminated in the red pulp. (B) Magnification of the box from panel A, showing granular hemozoin disseminated in the red pulp within a lymphocytic-histiocytic population. (C) Granular dark brown to black hemozoin was disseminated in the Kupffer cells of the liver. (D) Magnification of the box from panel C.

the SIV-only group, due to missing values. Plasma viral RNA values from 5 historical age-matched SIV control animals were included due to the low number ($n = 2$) of concurrent SIV control animals. The historical SIV-positive animals were also infected intravenously.

Differences in gametocytemia between *P. fragile* ($n = 6$) and SIV-*P. fragile*-coinfected animals ($n = 5$) over various time periods were assessed by the Wilcoxon rank-sum test statistic. Significance of the statistic was assessed by permutation methods, i.e., by considering all possible ways 5 of the 11 animals could have randomly been assigned to be coinfected. A similar analysis was applied to determine differences between *P. fragile* and SIV-*P. fragile*-coinfected animals in (i) percent infectivity, defined as the proportion of mosquitoes infected, and (ii) the number of oocysts per infected mosquito. A mosquito was considered infected if the midgut contained at least one oocyst.

For all analyses, one-sided *P* values were computed because of the lack of power with such small sample sizes and the *a priori* hypotheses that change in viral load, gametocytemia, and infectivity would be greater in coinfected animals. All statistical analyses were carried out using SAS v9.2 (SAS Institute, Cary, NC), StatXact 8 (Cytel Inc., Cambridge, MA), and R (www.R-project.org).

RESULTS

Development of a SIV-*P. fragile* coinfection model. We sought to develop a SIV-malaria coinfection model in the rhesus macaque because SIV infection in rhesus macaques is an accepted model of HIV pathogenesis. Among the simian parasites that generate *P. falciparum*-like infections, *P. fragile* was chosen for the development of a coinfection model because the clinical symptoms resemble *P. falciparum* infection in humans, it can be manipulated to develop as a chronic infection, it can be cultured *in vitro*, it has been previously used for drug studies, and it is noninfectious to humans (11, 13, 16).

Based on previous reports (16, 21), rhesus macaques were infected intravenously with *P. fragile*-infected erythrocytes. Peripheral parasitemia was determined by thin blood smear analysis (Fig. 1). Primary parasitemia developed within 14 days postinoculation of *P. fragile* (DPI-*P. fragile*) and was associated with a decrease in hematocrit and a transient fever (Fig. 1A). In one animal, 33959, *P. fragile*-infected red blood cells could not be detected during the first 2 weeks, and the animal therefore received a second inoculation with *P. fragile*-infected erythrocytes on day 14 after the first *P. fragile* infection. Parasitemia unexpectedly rose to >6% within 3 days after the second inoculation. As low parasitemia in *P. falciparum*-infected humans can be missed by blood smear analysis (38), we developed a quantitative PCR for the detection of *P. fragile* DNA. Indeed, retroactive PCR analysis of the blood sample obtained on day 11 after the first *P. fragile* inoculation confirmed that animal 33959 was positive by PCR for *P. fragile* although no *P. fragile*-infected red blood cells could be detected by blood smear analysis (see Fig. S1 in the supplemental material). Higher sensitivity of *P. fragile* detection by PCR is observed when data are presented as *P. fragile* copies per μl of blood, and highly congruent data of PCR and blood smear analysis were obtained when *P. fragile* detection was reported as infection of RBC (Fig. 1). Both methods were subsequently applied to determine parasitemia. To establish a persistent *P. fragile* infection, animals were treated with a subcurative dose of 150 mg of quinine sulfate on two consecutive days when parasitemia rose above 0.5% (Fig. 1A). This treatment resulted in a stabilization of the hematocrit and low but persis-

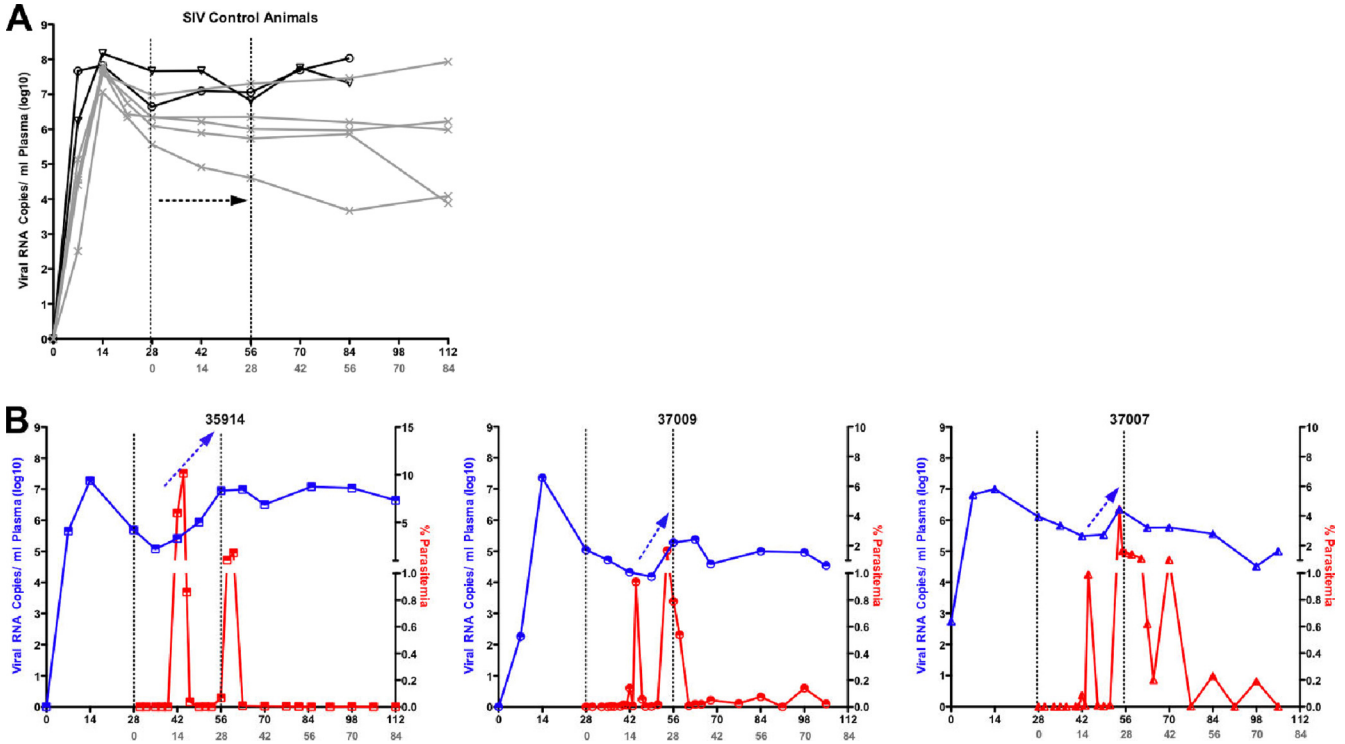

FIG. 3. Transient increases in viremia during acute malaria. (A) Longitudinal SIV RNA levels in SIV-infected animals. Concurrent and historical SIV-infected animals are represented by black open symbols and by the gray x, respectively. (B) Temporal correlation of viral RNA (blue) and blood smear parasitemia (red) for SIV-*P. fragile*-coinfected animals. Note the increase in the viral RNA slope between days 42 and 56 PI-SIV (black arrows).

tent parasitemia reflected in periodic spikes in peripheral parasitemia (Fig. 1A).

In a first attempt to determine the effect of *P. fragile* infection on the virological outcome in SIV-infected macaques, we infected animals with SIV 1 month prior to *P. fragile* infection. The virological parameters of SIV infection in rhesus macaques are well established, with peak viremia occurring within the first 7 to 14 days postinoculation with SIV (DPI-SIV) and the viral set point established between 28 and 56 DPI-SIV. Based on our results from animals infected with *P. fragile* only, we expected acute parasitemia to coincide with the establishment of viral set point. Indeed, SIV-infected animals exhibited peripheral parasitemia at approximately 14 DPI-*P. fragile*, at which time quinine sulfate treatment was initiated. However, despite an initial decline in parasitemia, the percentage of infected erythrocytes rose to 50% within 2 weeks of treatment (55 DPI-SIV), and the animals ($n = 2$) were humanely euthanized (Fig. 1B). This was direct evidence that coinfection altered clinical outcome, but this outcome is not reflective of the majority of coinfections that occur in humans. By extending the quinine sulfate treatment from 2 days to 4 days, we were able to effectively reduce parasitemia, stabilize the hematocrit, and establish chronic SIV-*P. fragile* coinfection (Fig. 1C).

At necropsy, pathological findings were similar between coinfected and *P. fragile*-only-infected animals. Gross findings were dominated by a marked diffuse splenomegaly. Histologically, there was mild to marked lymphofollicular hyperplasia in the spleen and in sampled lymph nodes (Fig. 2A). In addition, dark brown to black granular hemozoin was present throughout the red pulp in the spleen and in the Kupffer cell cytoplasm in the liver (Fig. 2). The liver also occasionally exhibited extramedullary hematopoiesis, represented by increased sinusoidal cellularity. Histological analysis of brain sections did not reveal any lesions or evidence of *P. fragile* cytoadherence (data not shown). However, animals were followed only for 3 months, and quinine sulfate treatment may have been sufficiently effective in preventing cerebral malaria.

Acute malaria transiently increased viremia in coinfected animals. Consistent with previous results (35), the SIV-infected macaques developed peak viremia within the first 7 to 14 DPI-SIV and reached the viral set point by week 6 postinoculation (Fig. 3A). In contrast, in SIV-*P. fragile*-coinfected macaques, a transient 1- to 2-log increase in plasma viral RNA copies was observed once acute parasitemia developed (Fig. 3A and B). Importantly, there was a statistically significant difference ($P = 0.001$) in the slope of plasma viral RNA between 42 and 56 DPI-SIV between SIV-only and SIV-*P. fragile*-coinfected macaques.

We hypothesized that the increase in viremia might be associated with immune activation induced by *P. fragile* infection. In fact, primary parasitemia resulted in a marked increase of activated $CD4^+$ T cells as measured by expression of Ki67 and CCR5 (Fig. 4A; see also Fig. S2A in the supplemental material). Importantly, there was a temporal overlap between the increase of $CCR5^+$ $CD4^+$ T cells, potential target cells of SIV, during the acute phase of *P. fragile* infection and the increase in viremia in SIV-*P. fragile*-coinfected animals (Fig. 4A). In addition, concurrent with

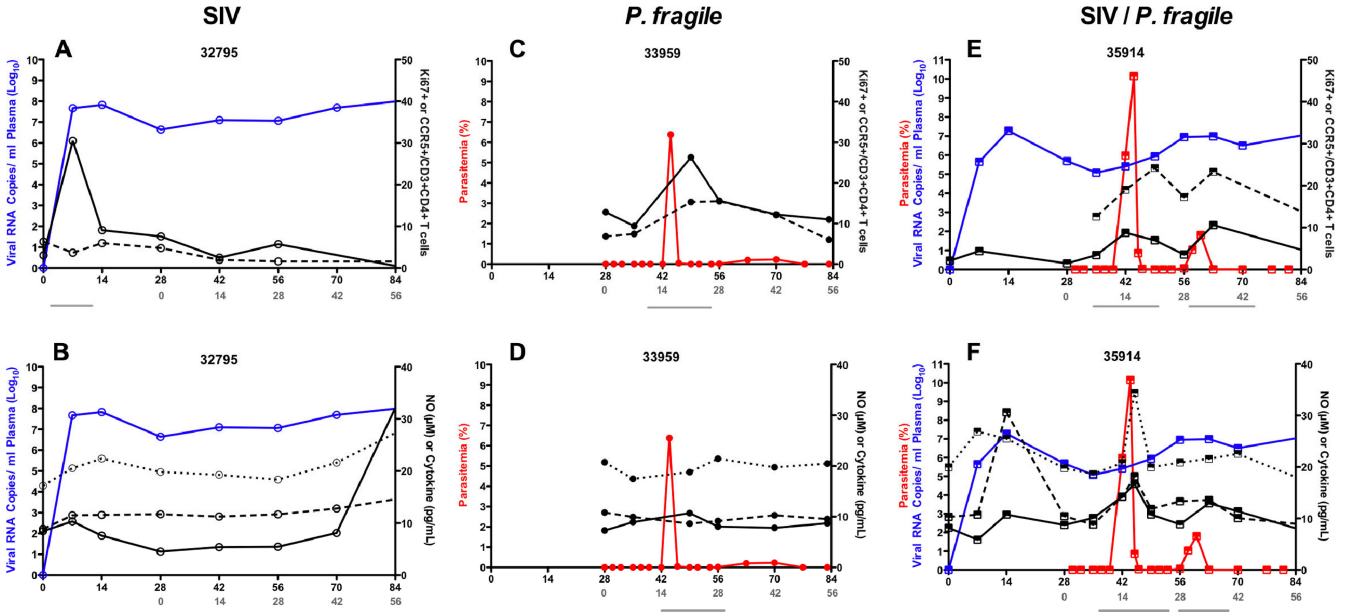

FIG. 4. Immune activation upon *P. fragile* infection in coinfected animals. (A) Percentage of $Ki67^+$ (dashed black line) or $CCR5^+$ (solid black) cells in the $CD3^+$ $CD4^+$ T cell population in relation to viremia (blue line) and/or parasitemia (red line) over time in representative SIV-only-infected, *P. fragile*-only-infected, and SIV-*P. fragile*-coinfected animals. (B) NO (solid black line), IFN-γ (dotted black line), and IL-6 (dashed black line) levels in relation to viremia and/or parasitemia as described above. Lines below the *x* axis indicate concurrent rises in parasitemia and activation markers.

the rise of parasitemia, plasma NO levels were elevated (Fig. 4B; see also Fig. S2B). Similarly, we noted an increase in plasma levels of the proinflammatory cytokines IL-6 and IFN-γ. This systemic immune activation induced by *P. fragile* infection coincided temporally with increased frequencies of activated $CD4^+$ T cells and increased viremia in SIV-*P. fragile*-coinfected animals (Fig. 4; see Fig. S2).

Coinfection enhances the transmission risk of malaria. There were no obvious differences in peripheral parasitemia between *P. fragile*-only and coinfected animals. Importantly though, only gametocytes, the sexual stages that are infective to mosquitoes, are important in malaria transmission. The factors triggering gametocyte development are unclear, but young erythrocytes and reticulocytes have been implicated in gametocyte development both experimentally and in field studies (33, 41, 42). Indeed, in both the *P. fragile*-infected and SIV-*P. fragile*-coinfected animals, we observed an increase in the percentage of gametocytes, both absolute and relative to total parasite number, during the initial drop in hematocrit (see Fig. S3 in the supplemental material). The increase in gametocytemia was confirmed by molecular analysis. The molecular quantitation of gametocytes was based on the fact that the switch from the asexual to the sexual stage of the parasite is associated with the expression of distinct genes. However, the sexual stage-specific genes for *P. fragile* have not been described. *P. fragile* (despite causing clinical symptoms similar to *P. falciparum* in humans) is genetically closely related to *P. vivax*. Based on known sexual stage-specific genes for *P. vivax*, we were able to clone a *P. fragile*-specific sequence and developed a real-time PCR method to complement the microscopic analysis for gametocytemia (see Fig. S1 in the supplemental material).

There was higher gametocytemia on days 14 to 27 after *P. fragile* infection (42 to 55 DPI-SIV) in SIV-*P. fragile*-coinfected animals relative to animals infected with *P. fragile* only ($P = 0.05$) (Fig. 5C, left panel). Because mosquitoes can become infected following feeding on blood that lacks microscopically detectable sexual-stage parasites and because detectable gametocytemia does not always equate with mosquito infectivity (18), we directly tested whether infectivity differed between *P. fragile*-infected and SIV-*P. fragile*-coinfected animals through *ex vivo* mosquito feeding on peripheral blood. The proportion of mosquitoes infected (i.e., with at least one oocyst in the midgut) was comparable between *P. fragile*-only and coinfected animals, except at 42 to 55 DPI-*P. fragile*, when coinfected animals had a higher percentage of infectivity ($P = 0.07$) (Fig. 5C, middle panel). Infected mosquitoes feeding on blood from the SIV-*P. fragile* group had more oocysts per midgut at 0 to 13, 14 to 27, and 28 to 41 DPI-*P. fragile* ($P \leq 0.10$) (Fig. 5C, right panel). As malaria is a vector-borne disease, the measurement of oocysts in mosquito midguts is a valid surrogate to assess transmission risk.

DISCUSSION

We developed a novel rhesus macaque model of SIV-*P. fragile* coinfection to study HIV-1-*P. falciparum* coinfection in humans. Our data demonstrate a transient increase of SIV replication during the acute *P. fragile* infection period in coinfected animals relative to animals infected with a single pathogen. The rise in viremia was associated with elevated cellular and systemic immune activation that may drive viral replication (Fig. 6). Furthermore, oocyst development was enhanced in mosquitoes that fed on blood from SIV-*P. fragile*-coinfected animals compared to blood from *P. fragile*-only-infected animals. These phenomena suggest that coin-

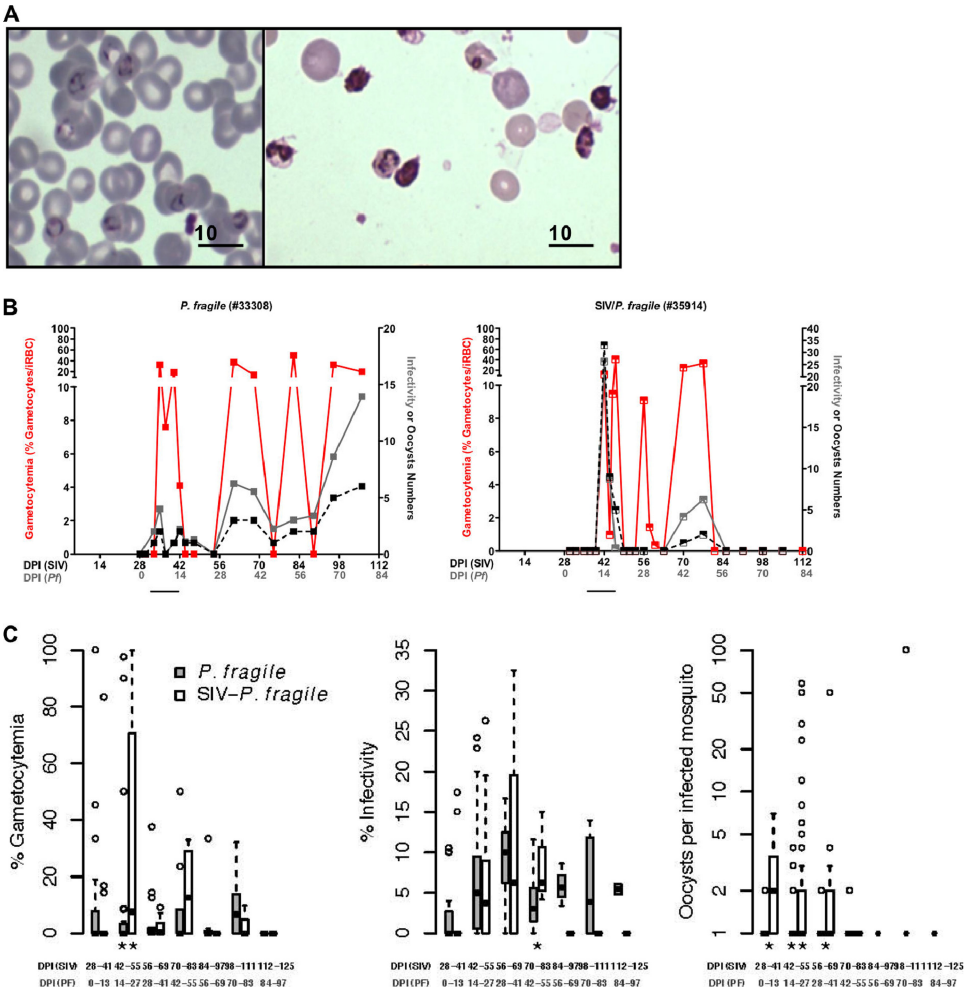

FIG. 5. Gametocytemia and mosquito infectivity. (A) Blood smears of *P. fragile*-infected erythrocytes with ring-stage parasites (left) and increased gametocytes in a representative SIV-*P. fragile*-coinfected animal (right). (B) Examples of the relationship between blood smear gametocytemia (red line), mosquito infectivity (gray line), and oocyst frequencies in mosquitoes (black line) over time in representative *P. fragile*-infected and SIV-*P. fragile*-coinfected animals, respectively. (C) Box plots of gametocytemia (left), percent infectivity (middle), and oocysts per infected mosquito (right) between *P. fragile* and SIV-*P. fragile*-coinfected animals. $**$, $P \leq 0.05$; $*$, $0.05 < P \leq 0.10$.

fection results in a higher risk of transmission of both HIV-1 and malaria.

Our model is most consistent with HIV-malaria coinfections in areas of unstable malaria, where malaria is more severe due to lack of preexisting immunity. Similarly, it would apply to infants infected with HIV by mother-to-child transmission prior to malaria infection. We acknowledge that the majority of HIV-malaria coinfections in humans are likely due to re-

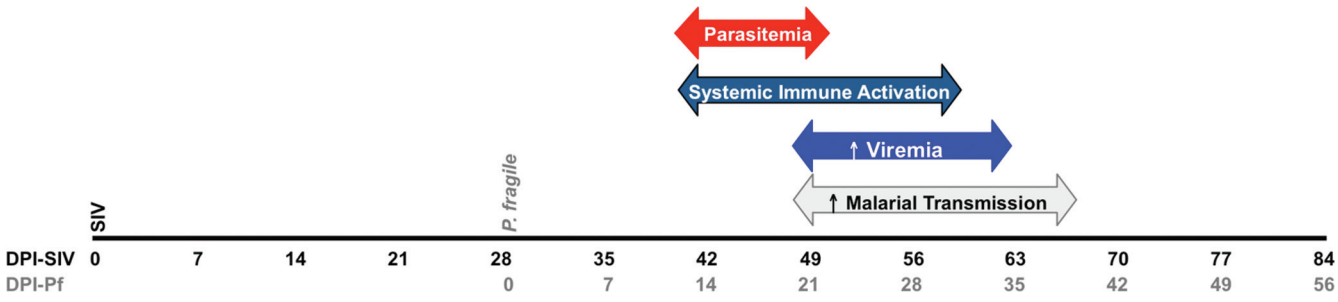

FIG. 6. Temporal relationship between immune, virological, and parasitological parameters in SIV-*P. fragile*-coinfected animals. SIV-infected macaques subsequently infected with *P. fragile* exhibited acute parasitemia and concurrent systemic immune activation. This activation could drive viral replication and provide more target cells for SIV, thereby elevating viremia. Coinfected macaques also exhibited increased malarial transmission compared to *P. fragile*-only-infected macaques during this acute infection period.

peated malaria infection beginning in early childhood, followed by HIV infection during adolescence. The SIV-*P. fragile* coinfection model described here is a novel model and as such was developed based on a wealth of data on the well-accepted SIV infection model of HIV infection in humans. Having successfully established this model, it can now be expanded to test the various scenarios of HIV-*P. falciparum* coinfection in humans.

During the initial rise in peripheral parasitemia of acute malaria infection, we observed a transient increase in viremia in coinfected animals, a trend which has been observed in human coinfections (5, 24, 28). Even an only slightly and/or transiently increased risk of HIV could have tremendous consequences in areas of high disease incidence. Thus, understanding of the underlying mechanisms that promote more severe pathogenesis and potential higher transmission rates is essential. We present evidence that immune activation, as assessed by increased frequencies of $Ki67^+$ and $CCR5^+$ $CD4^+$ T cells, and also by elevated systemic levels of NO and proinflammatory cytokines, is induced by *P. fragile* and is associated with a transient increase in viremia. We hypothesize that increased numbers of $CCR5^+$ $CD4^+$ T cells translate into higher numbers of target cells for the virus and that NO, through the activation of NF-κB, can directly induce HIV replication in virally infected cells (6, 39, 40, 51). In addition to affecting immune activation at this acute time point, we postulate that coinfected animals may experience heightened activation in the longer term that could promote earlier immune exhaustion and onset to simian AIDS. During the relatively short period of coinfection in the current study, pathological differences could not be detected between tissues of single and coinfected animals. Long-term studies of the coinfection model are warranted to follow the combined effect of malaria and SIV upon the immune system and clinical outcome.

With regard to the effect of coinfection on malaria pathogenesis, the 2-day quinine sulfate treatment that was effective in establishing chronic malaria infection in *P. fragile*-only-infected animals was not sufficient to control acute parasitemia in acutely SIV-infected animals. SIV and HIV are known to affect many players in the immune system, and we hypothesize that SIV-induced immunosuppression resulted in the different treatment outcomes. SIV infects $CD4^+$ T cells, resulting in cell death, and leads to $CD8^+$ T cell exhaustion (36). Loss of T helper function will impair multiple aspects of the host immune response. We observed that the chronically coinfected animals produced a less robust, although not significant, antimalarial humoral response than the chronically infected *P. fragile* animals (see Fig. S4 in the supplemental material). Similar findings of impairment of humoral immunity against malarial parasites were reported in the SIV-*P. cynomolgi* study and in pregnant coinfected women, suggesting SIV/HIV plays a role in diminishing the antibody response (26, 32). However, at this early time after SIV infection, impaired innate factors likely contributed to the lack of control of parasitemia. It is well known that dendritic cell frequencies and function are already reduced in acute HIV and SIV infection (7, 17). Similarly, *Plasmodium* spp. are known to directly alter dendritic cell function (31, 45). Coinfection with SIV and *P. fragile* may compound the immunologic damage induced by each pathogen, leading to more severe morbidity and pathology in coinfected individuals.

A key finding of our study was that coinfected animals exhibited higher gametocytemia during acute *P. fragile* infection than animals infected with *P. fragile* only. Importantly, during that same time period, oocyst development was significantly higher in mosquitoes that fed on blood obtained from SIV-*P. fragile*-coinfected animals than mosquitos that fed on blood from *P. fragile*-only-infected animals. These data indicate a heightened transmission risk of malaria during acute parasitemia in coinfected individuals. Unlike our model of chronic malaria that was induced by subcurative quinine sulfate treatment to develop the SIV-*P. fragile* coinfection model, humans in areas of endemicity are continuously and repeatedly challenged with new infections. Therefore, we hypothesize that the elevated infectivity to mosquitoes we observed during acute infection could occur during every new infection in humans. This would significantly increase the overall effect of coinfection on transmission, a hypothesis that could be tested in the primate model via repeated inoculations of *P. fragile* after curing the initial parasite infection with a higher treatment dose (16).

It was beyond the scope of the current study to establish a causative relationship, but the temporal patterns observed (Fig. 6) clearly suggest that immune activation during the acute parasitemia period in SIV-infected macaques was associated with the transient increase in viremia and enhanced mosquito infectivity. Thus, the data indicate that the transmission risks of both SIV/HIV and malaria are increased in coinfected individuals, at least during certain phases of coinfection.

The current study describes the development and key clinical and immunologic features of SIV-*P. fragile* coinfection. Future studies with larger numbers of animals and various temporal patterns of coinfection are required to further develop our understanding of HIV-malaria coinfection in humans. This model will likely provide a useful tool in defining the underlying immune mechanisms leading to disease exacerbation in coinfected individuals and in the design of novel therapeutics and vaccines to combat HIV-malaria coinfection in humans.

ACKNOWLEDGMENTS

This work was supported by the NIH research grants R21AI077373 to K.A. and T32-AI060555, STAR, and VSTP to K.T. We acknowledge the support of the UNC CFAR Biostatistics Core by grant number 5 P30 AI050410-12 (NIAID). All animal work was made possible through the support of the CNPRC by NIH/NCRR grant P51 RR00169-41.

We are grateful for expert technical help by Joyce Lee and Zachary Abbot.

K.A. and S.L. conceived and designed the experiments. W.C. and J.A.S. provided intellectual input and reagents for the experiments. Experiments were carried out by K.T., J.C., and R.T. Data were analyzed by K.T., J.C., S.L., K.A., C.K.M., M.G.H., and J.F. The manuscript was prepared by K.T., S.L., and K.A.

REFERENCES

1. **Abel, K., et al.** 2006. Rapid virus dissemination in infant macaques after oral simian immunodeficiency virus exposure in the presence of local innate immune responses. J. Virol. **80:**6357–6367.
2. **Abel, K., D. M. Rocke, B. Chohan, L. Fritts, and C. J. Miller.** 2005. Temporal and anatomic relationship between virus replication and cytokine gene expression after vaginal simian immunodeficiency virus infection. J. Virol. **79:**12164–12172.

3. **Abu-Raddad, L. J., P. Patnaik, and J. G. Kublin.** 2006. Dual infection with HIV and malaria fuels the spread of both diseases in sub-Saharan Africa. Science **314:**1603–1606.
4. **Aikawa, M., et al.** 1992. *Plasmodium coatneyi*-infected rhesus monkeys: a primate model for human cerebral malaria. Mem. Inst. Oswaldo Cruz **87**(Suppl. 3)**:**443–447.
5. **Ariyoshi, K., M. Schim van der Loeff, N. Berry, S. Jaffar, and H. Whittle.** 1999. Plasma HIV viral load in relation to season and to *Plasmodium falciparum* parasitaemia. AIDS **13:**1145–1146.
6. **Blond, D., et al.** 1998. Nitric oxide synthesis during acute SIVmac251 infection of macaques. Res. Virol. **149:**75–86.
7. **Brown, K. N., A. Trichel, and S. M. Barratt-Boyes.** 2007. Parallel loss of myeloid and plasmacytoid dendritic cells from blood and lymphoid tissue in simian AIDS. J. Immunol. **178:**6958–6967.
8. **Chandramohan, D., and B. M. Greenwood.** 1998. Is there an interaction between human immunodeficiency virus and *Plasmodium falciparum*? Int. J. Epidemiol. **27:**296–301.
9. **Chin, W., D. Moss, and W. E. Collins.** 1979. The continuous cultivation of *Plasmodium fragile* by the method of Trager-Jensen. Am. J. Trop. Med. Hyg. **28:**591–592.
10. **Cline, A. N., J. W. Bess, M. Piatak, Jr., and J. D. Lifson.** 2005. Highly sensitive SIV plasma viral load assay: practical considerations, realistic performance expectations, and application to reverse engineering of vaccines for AIDS. J. Med. Primatol. **34:**303–312.
11. **Coatney, G. R., W. E. Collins, M. Warren, and P. G. Contacos.** 1971. The primate malarias. CDC, Division of Parasitic Diseases, Atlanta, GA.
12. **Cohen, C., et al.** 2005. Increased prevalence of severe malaria in HIV-infected adults in South Africa. Clin. Infect. Dis. **41:**1631–1637.
13. **Collins, W. E., W. Chin, and J. C. Skinner.** 1979. *Plasmodium fragile* and *Macaca mulatta* monkeys as a model system for the study of malaria vaccines. Am. J. Trop. Med. Hyg. **28:**948–954.
14. **Collins, W. E., J. R. Jumper, C. S. Smith, and J. C. Skinner.** 1977. The exoerythrocytic stages of *Plasmodium fragile* in *Macaca mulatta* monkeys. J. Parasitol. **63:**226–231.
15. **Collins, W. E., et al.** 1994. Protective immunity induced in squirrel monkeys with recombinant apical membrane antigen-1 of *Plasmodium fragile*. Am. J. Trop. Med. Hyg. **51:**711–719.
16. **Collins, W. E., et al.** 2006. Studies on sporozoite-induced and chronic infections with *Plasmodium fragile* in *Macaca mulatta* and New World monkeys. J. Parasitol. **92:**1019–1026.
17. **Donaghy, H., B. Gazzard, F. Gotch, and S. Patterson.** 2003. Dysfunction and infection of freshly isolated blood myeloid and plasmacytoid dendritic cells in patients infected with HIV-1. Blood **101:**4505–4511.
18. **Drakeley, C., C. Sutherland, J. T. Bousema, R. W. Sauerwein, and G. A. Targett.** 2006. The epidemiology of *Plasmodium falciparum* gametocytes: weapons of mass dispersion. Trends Parasitol. **22:**424–430.
19. **Eyles, D. E.** 1950. A stain for malarial oocysts in temporary preparations. J. Parasitol. **36:**501.
20. **French, N., et al.** 2001. Increasing rates of malarial fever with deteriorating immune status in HIV-1-infected Ugandan adults. AIDS **15:**899–906.
21. **Fujioka, H., et al.** 1994. A nonhuman primate model for human cerebral malaria: rhesus monkeys experimentally infected with *Plasmodium fragile*. Exp. Parasitol. **78:**371–376.
22. **Grimwade, K., et al.** 2004. HIV infection as a cofactor for severe falciparum malaria in adults living in a region of unstable malaria transmission in South Africa. AIDS **18:**547–554.
23. **Hay, S. I., C. A. Guerra, A. J. Tatem, A. M. Noor, and R. W. Snow.** 2004. The global distribution and population at risk of malaria: past, present, and future. Lancet Infect. Dis. **4:**327–336.
24. **Hoffman, I. F., et al.** 1999. The effect of *Plasmodium falciparum* malaria on HIV-1 RNA blood plasma concentration. AIDS **13:**487–494.
25. **Hofmann, W., et al.** 1999. Species-specific, postentry barriers to primate immunodeficiency virus infection. J. Virol. **73:**10020–10028.
26. **Koehler, J. W., et al.** 2009. Altered immune responses in rhesus macaques co-infected with SIV and *Plasmodium cynomolgi*: an animal model for coincident AIDS and relapsing malaria. PLoS One **4:**e7139.
27. **Korenromp, E. L., et al.** 2005. Malaria attributable to the HIV-1 epidemic, sub-Saharan Africa. Emerg. Infect. Dis. **11:**1410–1419.
28. **Kublin, J. G., et al.** 2005. Effect of *Plasmodium falciparum* malaria on concentration of HIV-1-RNA in the blood of adults in rural Malawi: a prospective cohort study. Lancet **365:**233–240.
29. **Ljungstrom, I., H. Perlmann, M. Schlichtherle, A. Schert, and M. Wahlgren.** 2004. Methods in malaria research, 4th ed. Malaria Research and Reference Reagent Resource Center/ATCC, Manassas, VA.
30. **Marthas, M. L., et al.** 2011. Partial efficacy of a VSV-SIV/MVA-SIV vaccine regimen against oral SIV challenge in infant macaques. Vaccine **29:**3124–3137.
31. **Millington, O. R., C. Di Lorenzo, R. S. Phillips, P. Garside, and J. M. Brewer.** 2006. Suppression of adaptive immunity to heterologous antigens during Plasmodium infection through hemozoin-induced failure of dendritic cell function. J. Biol. **5:**5.
32. **Mount, A. M., et al.** 2004. Impairment of humoral immunity to *Plasmodium falciparum* malaria in pregnancy by HIV infection. Lancet **363:**1860–1867.
33. **Nacher, M., et al.** 2002. Decreased hemoglobin concentrations, hyperparasitemia, and severe malaria are associated with increased *Plasmodium falciparum* gametocyte carriage. J. Parasitol. **88:**97–101.
34. **Owens, C. M., P. C. Yang, H. Gottlinger, and J. Sodroski.** 2003. Human and simian immunodeficiency virus capsid proteins are major viral determinants of early, postentry replication blocks in simian cells. J. Virol. **77:**726–731.
35. **Parker, R. A., M. M. Regan, and K. A. Reimann.** 2001. Variability of viral load in plasma of rhesus monkeys inoculated with simian immunodeficiency virus or simian-human immunodeficiency virus: implications for using nonhuman primate AIDS models to test vaccines and therapeutics. J. Virol. **75:**11234–11238.
36. **Petrovas, C., et al.** 2007. SIV-specific CD8+ T cells express high levels of PD1 and cytokines but have impaired proliferative capacity in acute and chronic SIVmac251 infection. Blood **110:**928–936.
37. **Qari, S. H., Y. P. Shi, N. J. Pieniazek, W. E. Collins, and A. A. Lal.** 1996. Phylogenetic relationship among the malaria parasites based on small subunit rRNA gene sequences: monophyletic nature of the human malaria parasite, *Plasmodium falciparum*. Mol. Phylogenet. Evol. **6:**157–165.
38. **Schneider, P., et al.** 2005. Real-time nucleic acid sequence-based amplification is more convenient than real-time PCR for quantification of *Plasmodium falciparum*. J. Clin. Microbiol. **43:**402–405.
39. **Torre, D., and G. Ferrario.** 1996. Immunological aspects of nitric oxide in HIV-1 infection. Med. Hypotheses **47:**405–407.
40. **Torre, D., A. Pugliese, and F. Speranza.** 2002. Role of nitric oxide in HIV-1 infection: friend or foe? Lancet Infect. Dis. **2:**273–280.
41. **Trager, W., and G. S. Gill.** 1992. Enhanced gametocyte formation in young erythrocytes by *Plasmodium falciparum* in vitro. J. Protozool. **39:**429–432.
42. **Trager, W., G. S. Gill, C. Lawrence, and R. L. Nagel.** 1999. *Plasmodium falciparum*: enhanced gametocyte formation in vitro in reticulocyte-rich blood. Exp. Parasitol. **91:**115–118.
43. **Tripathi, R., R. A. Vishwakarma, and G. P. Dutta.** 1997. Plasmodium fragile: efficacy of arteether (alpha/beta) against cerebral malaria model. Exp. Parasitol. **87:**290–292.
44. **UNAIDS.** 2008. AIDS epidemic update, December 2008. UNAIDS/WHO, Geneva, Switzerland. http://www.unaids.org/en/KnowledgeCentre/HIVData/GlobalReport/2008/.
45. **Urban, B. C., et al.** 1999. *Plasmodium falciparum*-infected erythrocytes modulate the maturation of dendritic cells. Nature **400:**73–77.
46. **Van Geertruyden, J. P., J. Menten, R. Colebunders, E. Korenromp, and U. D'Alessandro.** 2008. The impact of HIV-1 on the malaria parasite biomass in adults in sub-Saharan Africa contributes to the emergence of antimalarial drug resistance. Malar. J. **7:**134.
47. **Van Geertruyden, J. P., et al.** 2009. Impact of HIV-1 infection on the hematological recovery after clinical malaria. J. Acquir. Immune Defic. Syndr. **50:**200–205.
48. **Van Rompay, K. K., et al.** 2010. Immunogenicity of viral vector, prime-boost SIV vaccine regimens in infant rhesus macaques: attenuated vesicular stomatitis virus (VSV) and modified vaccinia Ankara (MVA) recombinant SIV vaccines compared to live-attenuated SIV. Vaccine **28:**1481–1492.
49. **Waters, A. P., D. G. Higgins, and T. F. McCutchan.** 1993. Evolutionary relatedness of some primate models of Plasmodium. Mol. Biol. Evol. **10:**914–923.
50. **Whitworth, J., et al.** 2000. Effect of HIV-1 and increasing immunosuppression on malaria parasitaemia and clinical episodes in adults in rural Uganda: a cohort study. Lancet **356:**1051–1056.
51. **Xiao, L., S. M. Owen, D. L. Rudolph, R. B. Lal, and A. A. Lal.** 1998. *Plasmodium falciparum* antigen-induced human immunodeficiency virus type 1 replication is mediated through induction of tumor necrosis factor-alpha. J. Infect. Dis. **177:**437–445.
52. **Zapata, J. C., et al.** 2002. Reproducible infection of intact *Aotus lemurinus griseimembra* monkeys by *Plasmodium falciparum* sporozoite inoculation. J. Parasitol. **88:**723–729.